ANALYSIS OF SYNCHROTRON RADIATION USING SYNRAD3D AND PLANS TO CREATE A PHOTOEMISSION MODEL

L. Boon, A. Garfinkel, Purdue University, West Lafayette, IN, USA
K. Harkay, ANL, Argonne, IL, USA

Abstract

Using current models of synchrotron radiation production and propagation, work is being done on a realistic photoelectron model from Retarding Field Analyzer (RFA) data. This proposed photoelectron production model will be better able to predict the level of electron cloud density in the vacuum chamber. In this paper SYNRAD3D is used to simulate the production and propagation of photon radiation in in International Linear Collider(ILC) Damping Rings. Analysis of this radiation with photon reflections off the chamber wall has been completed. This data will be used in the future to study photoelectron production as a function of parameters such as minimum absorbed photon energy and lattice element type. The results show that wigglers are regions which create the most photons and therefore have the ability to produce the most photoelectrons.

INTRODUCTION

SYNRAD3D provides a 3-dimensional model of synchrotron radiation, allowing a study of radiation reflection around the perimeter of the chamber as a function of the longitudinal position, s [1]. This program will allow us to study various antechamber designs and other photon absorbers. The final goal is to have a photoelectron model which includes photoelectron emission energy. Comparison will be made to the photoemission in various lattice elements such as dipoles and wigglers to RFA data.

SYNRAD3D

SYNRAD3D is an extension of SYNRAD, a 2-dimensional program which calculates the radiation on the inner and outer most point of the chamber wall. SYNRAD3D uses the Better Methodical Accelerator Design(BMAD) library [1]. SYNRAD3D is a photon production and propagation code, which tracks photons. It uses radiation integrals to determine the probable initial position and energy of a specified number of photons around the ring. It then tracks the photons as they move and reflect in the chamber. SYNRAD3D uses data from the Berkeley's Center for X-Ray Optics to determine the probability of reflection and absorption of each photon as a function of energy and grazing angle (seen in Figure 1 [2]) As seen in the figure the chamber wall is assumed to have an 8 nm Al_2O_3 (aluminum oxide) layer on an Al substrate with 2nm surface roughness. Currently all scatters are specular and elastic.

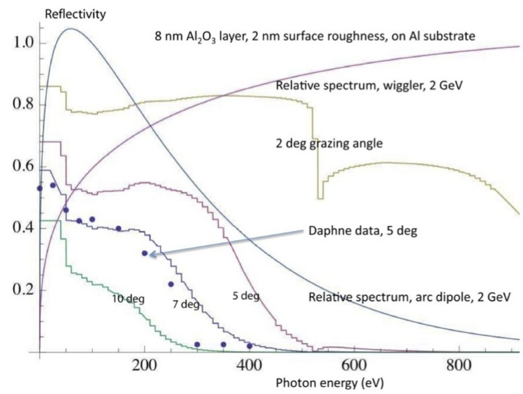

Figure 1: An example of the reflectivity of photons on a specified surface. The reflectivity is based on the photon energy and grazing angle. Data was taken from the Berkeley Center for X-Ray Optics [2] [1].

INTERNATIONAL LINEAR COLLIDER (ILC)

To decrease the cost of the ILC damping rings (DR) it has been proposed to decrease the circumference of the damping rings from 6.4 km to 3.2 km [4]. One of the concerns with a smaller ring is the build up of the electron cloud from photoemission and other effects.

A general schematic of the DR can be seen in figure 2 [4]. The main source of synchrotron radiation are wigglers (to cool the beam) and sector bends in the arcs. To make a better comparison of the photon flux between the current and proposed damping ring the first cut in data ignored all photons with energy less then 4 eV. 4eV was chosen because it is the work function for the chamber wall, which is Al. In addition to the energy cut all wiggler magnets are modeled as alternating dipoles and drifts. Normalization was done using equation 1.

$$\text{photons/m/beam particle} = \frac{N_L * I}{L} \quad (1)$$

L is the length of the section to average over, and N_L is the number of photons incident on the wall in length L [1]

Analysis for the 3.2 km proposed ring (DSB3)

For the analysis of the 3.2 km ring 101,000 photons were generated. Figure 3 a&b show the normalized photon flux along the inside and outside wall of the damping ring, respectively, where s = 0 is between the injection and extraction points as seen in Figure 2. The main feature of the

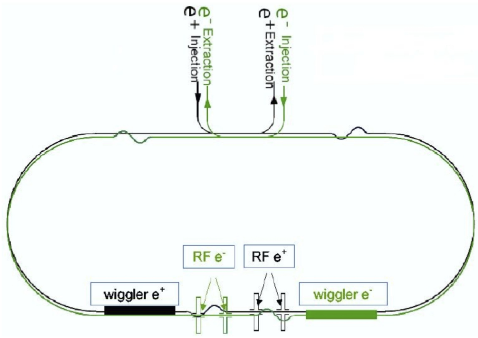

Figure 2: A schematic of the ILC damping ring. [4]

photon flux is a sharp spike at s = 2100. This heightened flux is created by the radiation in the wigglers that is radiated in the direction of the beam, this radiation is then absorbed directly downstream in the first dipole. Besides the photon spike at s = 2100m the inner and outer chamber walls receive similar amounts of photon radiation without antechambers present as seen in figure 4; a graph of the normalized photon radiation through the wigglers. Comparing Figure 4(a) and Figure 4(b) it can be seen that the photon flux for the wigglers on both the inside and outside wall of the chamber is the same when no antechamber is present.

The opening angle of the wiggler radiation with respect to the beam is defined by the equation:

$$\Psi = \begin{cases} 1/\gamma \left(\frac{\omega_c}{\omega}\right)^{1/3} & \omega << \omega_c \\ 1/\gamma & \omega = \omega_c \\ 1/\gamma \left(\frac{\omega_c}{\omega}\right)^{1/2} & \omega >> \omega_c \end{cases} \tag{2}$$

where Ψ is the opening angle, ω_c is the critical photon energy, ω is the energy of the photon, and γ is the relativistic gamma. For the ILC ω_c is —keV. Figures 5 & 6 compare the photon absorption distribution around the perimeter of the chamber wall in the wiggler(figure 5) and — after the wiggler(Figure 6). Zero has been defined as on the positive x-axis, with positive values above the axis x-axis and negative values below the x-axis. The narrow distribution seen in figure 5 corresponds to a smaller opening angle. Because photons are absorbed closer to the wiggler radiation source. Figure 6 is the distribution around the chamber at the high photon flux in the first dipole after the wigglers, at s = 2100m. The distribution around the zero point is wider here. This spread is consistent with the opening angle.

Analysis of the current 6.4 km ring(DCO4)

A similar analysis was completed of the 6.4 km ring so that a comparison between the two could be made. To keep the photons normalized with those of the smaller 3.2 km ring 560,000 photons were produced in the simulation.

The initial graphs of the entire ring show similar features as seen in the 3.2 km ring, with just a few differences in magnitude, compare figures 7 and 3. The main difference is in the photon spike after the wigglers. In the 3.2

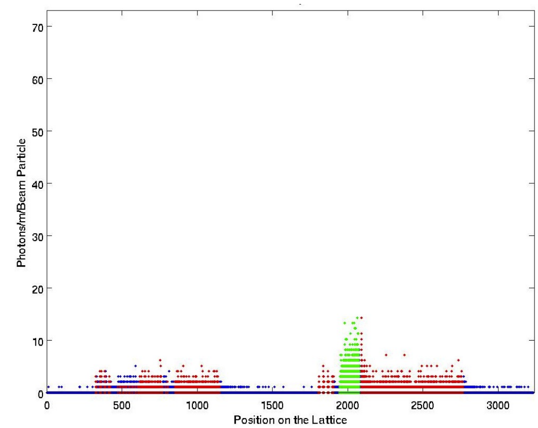

(a) Inside chamber wall

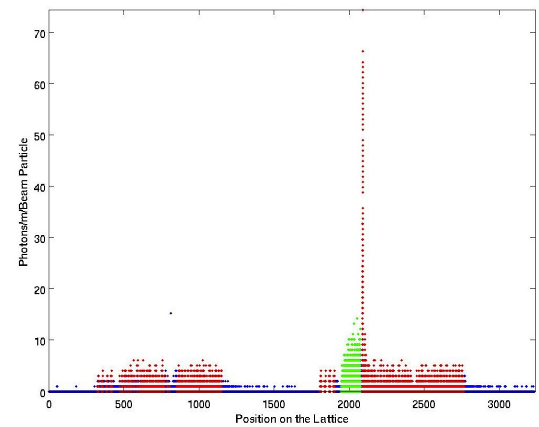

(b) Outside chamber wall

Figure 3: A graph of the photon flux along the inside and outside of the 3.2 km damping ring chamber wall, the individual photons have been normalized by equation 1

km ring the maximum value of photon flux reached is 72 photons/m/beam particle, while in the 6.4 km ring the flux is about half that at 37 photons/m/beam particle. The difference in photon flux is due to the shape of the ring, the smaller ring has a sharper turn in each of the dipoles so there are more photons incident on a shorter section of the ring then there are in the larger 6.4 km ring.

An analysis of the photon flux as a function of the perimeter yields the same results as the 3.2 km ring with respect to the opening angle of the generated photons. However similar the shape of the flux there is a higher flux of photons with higher energies than seen in the 3.2 km ring in both the wiggler and spike sections of the chamber wall. (not shown)

RETARDING FIELD ANALYZERS (RFA)

Retarding Field Analyzers [3] are detectors placed in the Advanced Photon Source (APS) and Cornell's CesrTA that measure the energy of free electrons in the chamber. In APS there were 10 detectors in one of the straight sections of the storage ring, the placement is seen in Figure 8. A

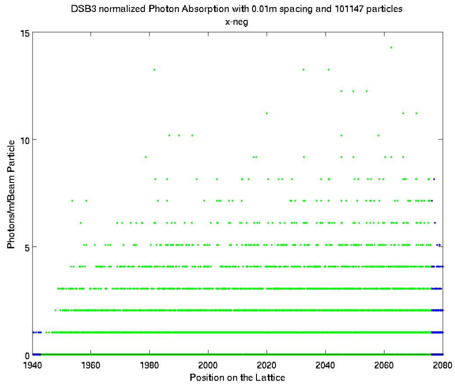

(a) Inside chamber wall

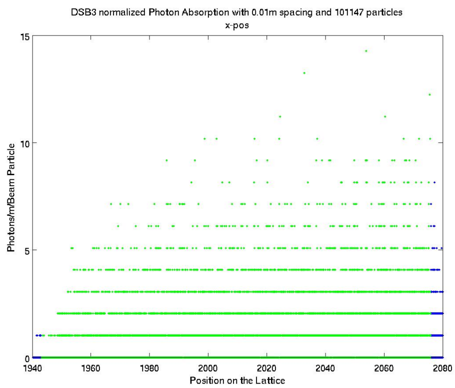

(b) Outside chamber wall

Figure 4: Zoomed in view of the photon flux in the wiggler for the inside and outside of the chamber wall. Both sides have the same photon flux when no antechamber is present.

schematic of the detector can be seen in Figure 9. It has a grounded plate to shield the beam, and a retarding voltage to allow only free electrons with a given energy to be detected.

Data was taken at APS in 1998 and 1999 for both positron and electron beams. The data is believed to fit a lorentzian function (Figure 10)

$$L = \frac{\frac{C_1\Gamma}{2}}{(\frac{\Gamma}{2})^2 + (E - \langle E \rangle)^2}. \quad (3)$$

However for detectors close to the end absorber (EA) such as detector 1, there appears to be a tail after the main peak which decreases more slowly than for data from detectors farther away from the EA. This can be seen in Figure 11. This extra shape is believed to be an exponential and currently an analysis program is being written to calculate the best fit for the sum of a lorentzian and exponential decay.

$$L = \frac{\frac{C_1\Gamma}{2}}{(\frac{\Gamma}{2})^2 + (E - \langle E \rangle)^2} + C_2 e^{-\frac{E}{C_3}} \quad (4)$$

Once this is complete the archived data from APS will be used to study the production of photoelectrons over time,

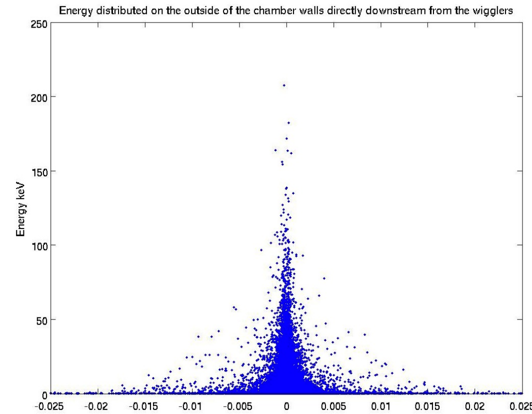

Figure 5: Photon flux along the chamber wall as a function of the perimeter in the wiggler, the tight peak indicates a small opening angle consistent with the photons being generated close to the location they were absorbed.

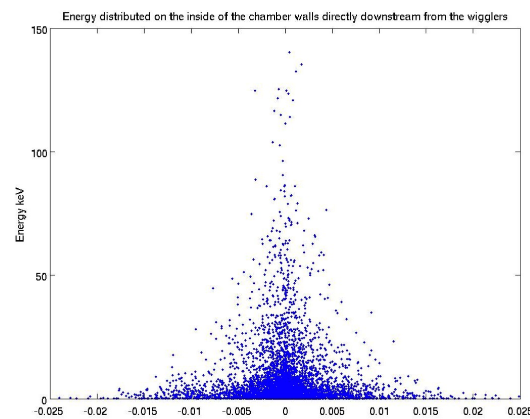

Figure 6: Photon flux along the chamber wall as a function of the perimeter in the photon flux spike near s = 2100m, the wide peak indicates a large opening angle consistent with the photons being generated far from the location they were absorbed.

and location relative to the EA. The fitted data will be used as input to a photoelectron model to be incorporated into SYNRAD3D. The RFA's near the EA most resemble the no-antechamber design analyzed earlier in this paper.

CONCLUSION/SUMMARY

Using SYNRAD3D synchrotron radiation models have been studied of both the current and proposed ILC DR. These models show that with the smaller ring there will be more photon flux in the wigglers and in the first dipole downstream from the wigglers. This can be reduced with the use of antechambers, but these simulations have not yet been done. The simulations presented here are consistent with theory. High energy photons are produced in the wigglers and have a small opening angle. The effect of the high photon flux will be studied further with the proposed

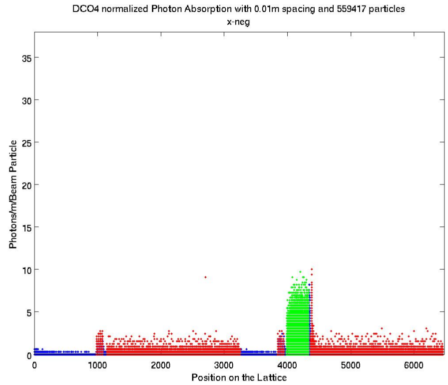

(a) Inside

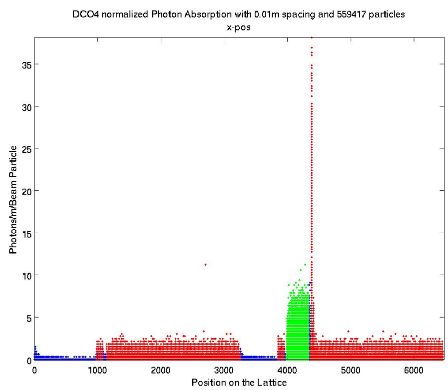

(b) outside

Figure 7: A graph of the photon flux along the inside and outside of the 6.4 km damping ring chamber wall, the individual photons have been normalized by equation 1

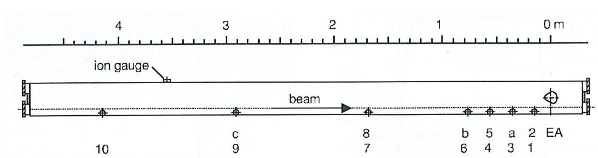

Figure 8: Location of the RFA detectors labeled 1-10 in the APS ring. [3] EA is an end absorber.

photoemission model being created.

ACKNOWLEDGEMENTS

The authors would like to thank D. Sagan and G. Dugan who write SYNRAD3D. And the entire electron cloud group based at Cornell University who gave feedback on this work as it progressed. Thanks also to thank M. Harrison, Director, ILC Global Design Effort Americas Regional Director for financial support.

This work is supported by U.S. Department of Energy, Office of Sciences under contract no. DE-AC02-06CH11357

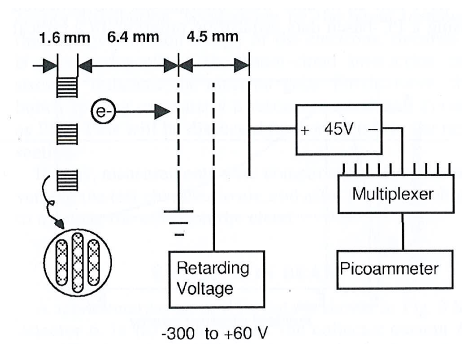

Figure 9: A schematic of the RFA detector. [3]

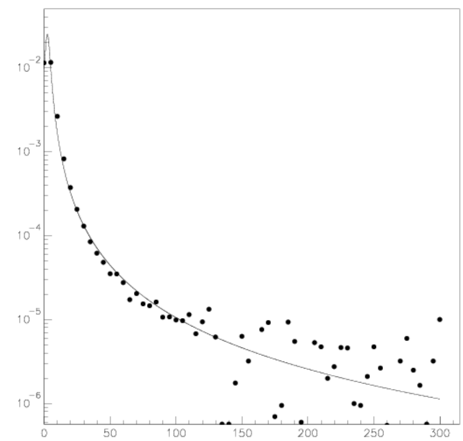

Figure 10: Demonstrates the lorentzian fit used to determine the peak electron energy generated by photons in detector 6.

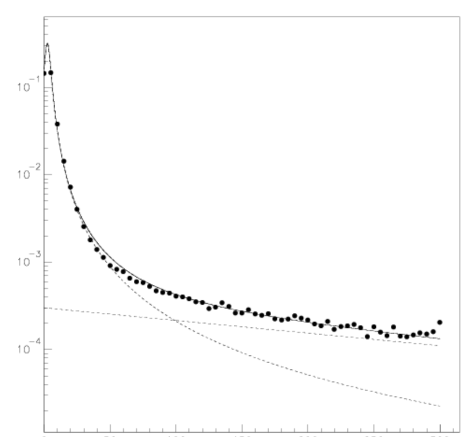

Figure 11: A plot of the readout from detector 1 (near the end absorber); notice need to add a second function to fit the data, this second function is an exponential decay. These added electrons are produced by the proximity to the EA.

REFERENCES

[1] Dugan, G., D, Sagan, ”Synrad3d photon propagation and scattering simulation”, ECLOUD10 proceedings.

[2] Gullikson, E. ”X-Ray Interactions With Matter”, http://henke.lbl.gov/optical_constants/mirror2.html

[3] Harkay, K., R. A. Rosenberg. ”Properties of the Electron Cloud in a High-Energy Positron and Electron Storage Ring” Physical Review Special Topics-Accelerators and Beams Vol 6, 034402, 2003

[4] Pivi, M. T. F., et al. ”Recommendation for the Feasibility of More Compact LC Damping Rings,” IPAC’10, Kyoto, Japan, May 2010, p. 3578, www.jacow.org.